J Mater Sci (2007) 42:6809–6818
DOI 10.1007/s10853-006-1426-4

Solute adsorption and exclusion studies of the structure of never-dried and re-wetted cellulosic fibres

R. N. Ibbett · S. Kaenthong · D. A. S. Phillips · M. A. Wilding

Received: 28 March 2006 / Accepted: 11 December 2006 / Published online: 27 April 2007

Abstract The total water capacity of a series of never-dried and re-wetted cellulosic fibres has been shown to correlate with the accessible volume described by a thermodynamic model. The model was applied to interpret the adsorption behaviour of a range of reactive dyes in electrolyte solutions and was successful in accounting for differences in fibre anionic charge. Comparative solute exclusion data indicated the existence of a population of very small spaces in never-dried cellulosic fibres, which may be associated with water disrupting the cellulose $1\bar{1}0$ crystal planes. Such intra-crystalline spaces may provide sites for uptake of planar substantive dyes and may also be accessible to sodium ions. The study showed that never-dried lyocell undergoes a large reduction in total wet capacity following initial drying, which is believed to be due to both exudation of crystal water and to inter-fibrillar crystallisation. This crystallisation mechanism may not be so effective for viscose and modal, which have poorer structural organization. Re-wetted lyocell exhibits high dye adsorption, which may result from the development of a uniform fibrillar morphology with a high surface area. This structural aspect is not expressed by the thermodynamic model.

Introduction

The never-dried state refers to the condition of a cellulosic fibre following the spinning and coagulation-regeneration manufacturing steps. The phase-separated polymer structure is washed to remove residual process liquor and the fibre is collected prior to the drying step. The microtexture of the fibre contains water filled spaces that collapse on drying, allowing consolidation of the cellulose structure through additional hydrogen bonding between polymer domains. Pore spaces within the consolidated structure will reopen as the fibre is re-wetted but the pore texture, cellulose crystallinity and extent of swelling may be irreversibly altered compared to the original never-dried state [1–3].

Earlier published work has demonstrated that the dye uptake of different cellulosic fibre products is higher in the never-dried state compared to the conventional re-wetted state [2, 4]. This appears to be especially true where large, high-substantivity, anionic dyes are considered, under exhaust conditions using low levels of electrolyte [4]. These findings suggest that efficiencies may be gained by applying effect chemicals in the never-dried condition, as a result of greater accessibility within the fibre structure. This could lead to savings in chemical utilization and production costs, or alternatively could lead to opportunities for the on-line manufacture of unique products, not realizable by treating commercial re-wetted fibre.

The influence of fibre structure on dye or chemical uptake has been the subject of many previous studies [3, 5, 6]. However, few of these investigations have considered the unique structure of the never-dried state and how this contrasts with the re-wetted state of the commercial fibre [1, 4, 7]. The properties of anionic dyestuffs have also been studied in detail, with respect to the structural and chemical factors influencing cellulose affinity [8–11]. However, the influence of the fibre morphology on dye affinity and accessibility has in the main been considered from a thermodynamic standpoint [12–14]. Other studies

R. N. Ibbett (✉) · S. Kaenthong · D. A. S. Phillips · M. A. Wilding
Christian Doppler Laboratory for Fibre and Textile Chemistry in Cellulosics, School of Materials, University of Manchester, Manchester M60 1QD, UK
e-mail: Roger.ibbett@manchester.ac.uk

have concentrated on the experimental determination of fibre texture and porosity, using techniques such as small-angle X-ray scattering and inverse size exclusion chromatography [15–18]. However, results have often been compared only on an empirical basis with dyeing behaviour [5, 19].

An opportunity exists for gaining improved understanding of the properties of never-dried and re-wetted fibre materials by comparing dye uptake data with that from complementary physical techniques. In this respect dyes can be considered as coloured molecular probes, providing insights into fibre internal pore structure and surface character. An attempt can then be made to combine both thermodynamic and structural concepts to try and rationalise differences observed between cellulosic fibre types.

This current study is partly concerned with the interpretation of adsorption data collected using a selection of reactive dyes applied to never-dried and re-wetted viscose, modal and lyocell cellulosic fibres, using neutral, low salt dye-bath conditions [4]. Reactive dyes are most commonly used for cellulosic fibre colouration, and their behaviour towards different substrates is of considerable commercial interest. Fibre porosity information has been gathered using a centrifugation technique and also by modeling solute-exclusion profiles obtained using an equilibrium static method [20, 21]. The measurement of free-state samples was considered most appropriate for study of the fine structure in the nascent never-dried condition. A thermodynamic model, was originally proposed by Peters and Vickerstaff, has been used to relate dye uptake to fibre porosity, accounting for solution electrolyte concentration and fibre anionic charge [12, 22–24]. This provides a new insight into fibre accessibility, which will be of value in the understanding of both never-dried and re-wetted phase morphologies.

Experimental

Fibre samples

Commercial dried samples of lyocell, viscose and modal fibres were supplied by Lenzing AG. These were all 1.3dtex, 38 mm staple-length products. In all future discussion these are referred to as the re-wetted samples, as immersion is required before all measurements. Corresponding never-dried materials were collected after the washing stage of production, following complete removal of spin-bath liquors. These were then sealed in water-tight bags and stored in a refrigerator (5 °C) before use. Handling of never-dried material was carried out carefully, so as to avoid moisture loss or mechanical damage.

Dye uptake

Five commercial monochloro-triazinyl type reactive dyes were selected, with differing sulphonate functionalities and with different adsorption behaviour towards cellulose. These were Procion Red HE3B (CI Reactive Red 120), Procion Red HE7B (CI Reactive Red 141), Procion Yellow HE4R (Reactive Yellow 84), Procion Orange HER (CI Reactive Orange 84), and Procion Navy HER (CI Reactive Blue 171). Dyeings were carried out under neutral exhaustion conditions with a liquor to fibre ratio of 20:1, at 80 °C, using a laboratory dyeing machine (Mathis AG). The restriction of the investigation to the neutral phase of dyeing ensured that uptake would be due only to physical adsorption and that chemical fixation effects could be discounted. Dye-baths were made up to a concentration equivalent to 1% by dye weight on fibre, using low electrolyte conditions by addition of 4 g/L of sodium chloride. Initial and final dye-bath concentrations were determined by visible spectroscopy, from a Beer's law absorbance relationship. Concentration values were used to calculate the final equilibrium concentration of dye on fibre [D_f] and remaining dye in the bath [D_s], with results for each dyeing expressed as a molar partition ratio ($P = [D_f]/[D_s]$). The purities of the commercial dyes were determined by titremetric reduction of the dye azo group, using titanous chloride solution [25]. The inorganic buffer in all commercial dye formulations was estimated to be 30% of total weight. In addition, it was assumed that under neutral conditions this electrolyte contribution to the thermodynamic model could be expressed on the basis of an equivalent weight of sodium chloride.

Centrifugation

Duplicate samples of both never-dried and dried (re-wetted) fibre were immersed in de-ionised water for 5 min, and then centrifuged for 15 min at 1400g. The fibres were supported in the centrifuge tube on a wire screen, which allowed the interstitial (non-pore water) to be drained away. The centrifuged fibres were weighed immediately, then dried in an oven at 105 °C to constant mass, then reweighed. The loss in mass on drying is expressed as the water retention (WR) per gram of dry fibre, which represents the quantity of water contained within the fine porous morphology of the saturated fibres [26].

Determination of carboxyl content

Samples of dry and never-dried fibres were added to a solution of 600 mg/L of methylene blue (CI Basic Blue 9) cationic dye (Sigma Diagnostic Inc.), buffered to pH 8.5, at a liquor to goods ratio 100:1, according to the method of

Davidson [27]. Dye-fibre liquors were continuously rotated for 20 h using the laboratory dyeing machine, at 25 °C, which was sufficient time to achieve adsorption equilibrium [28]. The visible absorbances of the dye liquors for each sample were measured initially and at equilibrium, which were used to determine the weight of methylene blue adsorbed per gram of dry fibre. Corrections were applied to account for fibre moisture and dye purity (specified as 99.5%). Assuming an acid–base adsorption mechanism, the molar quantity of dye taken up was assumed to correspond to the fibre carboxyl content, expressed in milliequivilants per gram.

Solute exclusion

A range of molecular weights of glycol, polyethylene glycol (PEG) and polyethylene oxide (PEO) polymers were used as probe molecules, all with narrow weight distributions (Sigma-Aldrich Co.). These were ethylene glycol, diethylene glycol, triethylene glycol, PEG200, 400, 600, 1000, 1500, 3400, 10000 and PEO100000. Initial polymer solutions were made up at 30 g/L, with accurate volumes of 20 mL of each solution added to weighed portions of approximately 4 g of fibre, in 50-mL bottles. After addition, the bottles were capped and shaken at intervals over a 24-h period, at ambient temperature. The refractive index of the initial polymer solutions and the final supernatent liquors from each bottle were determined using a carefully thermostatted refractometer (Bellingham Stanley Ltd.), ensuring that no fibre fragments from the liquors were transferred to the measurement window. The refractive index values were used in the appropriate calibration equations, to determine the change in PEG/PEO concentration, which relates to the extent of exclusion of the polymers from the fibre pore structure [29, 30].

In the case of never-dried fibres, the water contained either interstitially or within internal pores gave would be expected to cause a reduction in polymer concentration, depending on the extent of exclusion. For the re-wetted fibres, the effect of exclusion would raise the polymer concentration in the supernatent liquor, after taking account of the ambient regain of the samples. The same formulae were used in both cases for determining the inaccessible (excluded) volume (V_i) per gram of dry fibre for each PEG/PEO solute molecular size, according to Eq. 1, where C_i = initial solute concentration, C_f = final solute concentration, W = weight of initial solution (density assumed = 1), q = weight of water added with the fibre, and x = fibre dry weight.

$$V_i = \frac{(W+q)}{x} - \frac{WC_i}{xC_f} \quad (1)$$

The accessible volume of the fibre is then $V_a = (V_{max} - V_i)$, where V_{max} is the inaccessible volume of the largest probe molecule, representing the total saturated pore volume.

The apparent diameter (s) of the PEG/PEO solute probe was calculated using a formula proposed initially by Squire [31] according to Eq. 2, where M = weight average molecular weight.

$$s = 1.74(M)^{0.4} \quad (2)$$

Results

Dye partition ratios, water retention and carboxylate contents for all fibres are shown in Table 1. In all cases the values for never-dried samples have been expressed on a dry-weight equivalent basis.

The inaccessible volumes (V_i) from the solute exclusion experiments were first plotted against solute probe diameter (s), as illustrated for never-dried lyocell in Fig. 1.

Table 1 Equilibrium dye uptake, carboxyl analysis and total wet volumes of different cellulosic fibres

Dye	Partition ratio (P)					Carboxyl content [C]	Centrifuged water retention (WR)	Reduction in WR from never-dried to re-wetted
	Red 120	Red 141	Yellow 84	Orange 84	Blue 171			
			(kg/L)			(meq/g)	(mL/g)	(%)
Fibre sample								
Never-dried lyocell	134	202	34	37	147	28	1.06	
Never-dried viscose	37	22	5	5	23	55	1.01	
Never-dried modal	19	9	3	2	12	39	0.68	
Re-wetted lyocell	49	91	19	14	71	29	0.72	32
Re-wetted viscose	20	24	5	4	31	52	0.93	8
Re-wetted modal	10	8	2	2	9	38	0.63	7

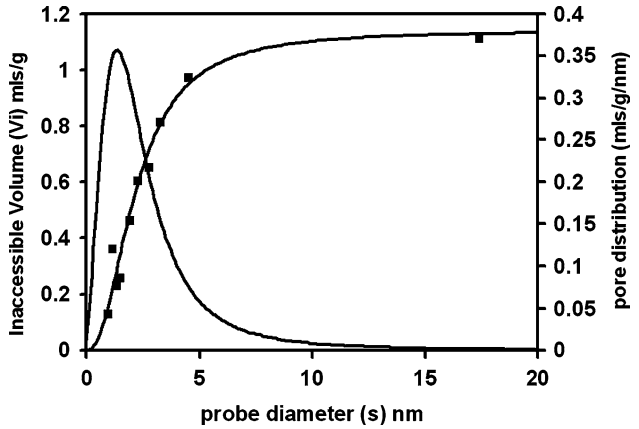

Fig. 1 Experimental plot of inaccessible volume (V_i) against PEG/PEO molecular diameter from solute exclusion data, for never-dried lyocell fibre, with cumulative and differential fitted functions

Best-fit trend lines were established using a Fisk type function, according to Eq. 3, where A, w and b are adjustable parameters, representing the maximum, width and bias of the function. Similar equations have been used in the past to describe exclusion curves and also size distributions of geological materials [29, 32]:

$$V_i(\text{function}) = \frac{As^b}{(w^2 + s^b)} \tag{3}$$

The best-fit value for the parameter (A) is equivalent to the saturation pore volume (V_{max}), which was then used to calculate the accessible volume (V_a) for all experimental points. Experimental and fitted values for (V_a) were plotted against solute probe size (s) for viscose, modal and lyocell fibre samples, as shown in Figs. 2–4.

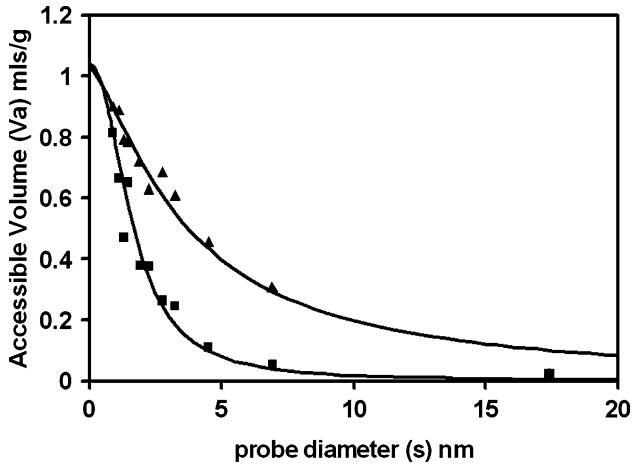

Fig. 2 Experimental and fitted distribution of wet-state accessible volume (V_a) from solute exclusion data, for never-dried (■) and re-wetted (▲) viscose fibre

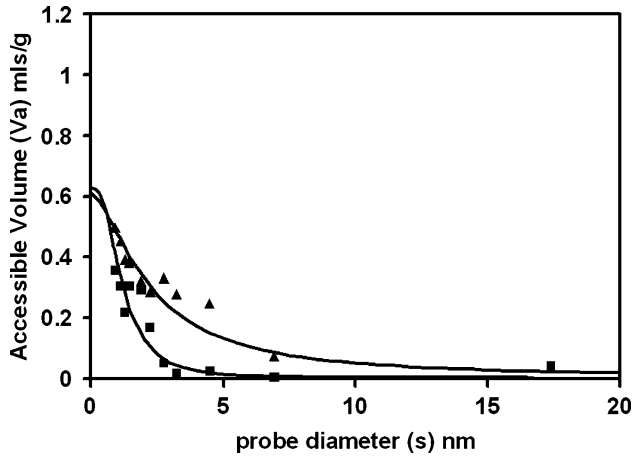

Fig. 3 Experimental and fitted distribution of wet-state accessible volume (V_a) from solute exclusion data, for never-dried (■) and re-wetted (▲) modal fibre

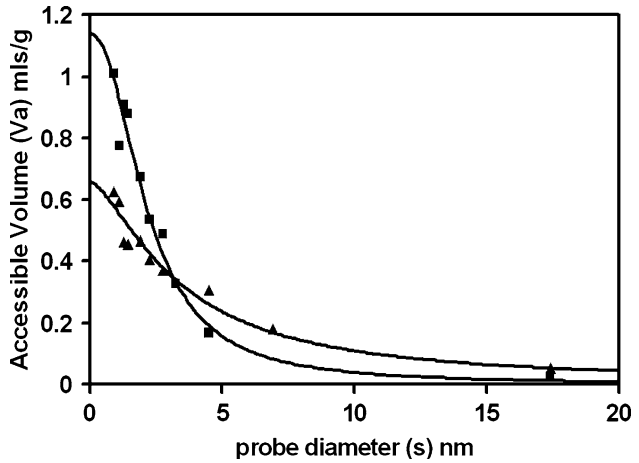

Fig. 4 Experimental and fitted distribution of wet-state accessible volume (V_a) from solute exclusion data, for never-dried (■) and re-wetted (▲) lyocell fibre

The volume average mean pore width for each fibre (s_m) is given by Eq. 4, where w and b are best-fit values of the original Fisk function. The size limit accounting for 95% of the pore volume was also calculated from the fitted function. Numerical differentiation was carried out to allow graphical determination of the peak (modal) pore size (s_p) and the peak height (h) of the distribution profile, as illustrated in Fig. 1. The integral breadth of the profile (B) was determined according to Eq. 5 and the average surface area (U) from Eq. 6, assuming lamellar geometry. The results for each fibre are summarised in Table 2.

$$s_m = w^{2/b} \tag{4}$$

$$B = A/h \tag{5}$$

$$U = 2A/m \tag{6}$$

Table 2 Solute exclusion of PEG/PEO by wet cellulosic fibres

Fibre sample	Mean pore size (s_m) (nm)	Peak Size (s_p) (nm)	Integral breadth of pore distribution (B) (nm)	Saturation volume (V_{max}) (mL/g)	Size limit accounting for 95% volume (s_{95}) (nm)	Surface area (U) (lamellar model) (m^2/g)
Never-dried lyocell	2.2	1.3	3.2	1.14	9	1035
Never-dried viscose	1.6	1.0	2.3	1.05	7	1338
Never-dried modal	1.2	0.9	1.6	0.63	4	1059
Dried lyocell	3.4	1.3	5.5	0.66	18	391
Dried viscose	3.7	1.2	6.0	1.03	12	557
Dried modal	2.2	1.0	3.7	0.61	14	546

Results from fitting of three-parameter Fisk function

The partition ratios for the selected dyes were applied as input parameters to the Peters and Vickerstaff model. According to their treatment, the free energy ($-\Delta G^\circ$) of the dye-cellulose interaction at dyeing equilibrium is expressed by Eq. 7, where the chemical activities (A_f) and (A_s) relate to the dye concentration in the fibre [D_f] and in solution [D_s], used to establish the experimental dye partition ratio (P) in Table 1. The sodium ion concentrations in the fibre [Na_f] and in solution [Na_s] are required for the ionic products, according to Eqs. 8 and 10, which can be found from the added salt concentration, or by use of Donnan ion partition theory, according to Eq. 9. The fibre anionic charge has a direct influence on the dye equilibrium and the values from the experimental carboxyl determinations were used to apply a correction within Eq. 9. The number of sulphonate groups attached for solubilisation account for the anionic charge of each dye (z). Finally, a fibre volume factor (V) must be used to convert the dye concentration in the fibre to units of mol/L, rather than the experimentally determined mol/g. This can be used to describe the internal volume of the fibre accessible to the dissolved dye molecule.

$$-\Delta G^\circ = RT \ln(A_f/A_s) \tag{7}$$

$$A_f = \frac{[D_f][Na_f]^z}{V^{z+1}} \tag{8}$$

$$[Na_f]_{cor} = 0.5\{z[D_f] + (z^2[D_f]^2 + 4V^2[Na_s][Cl_s])^{0.5}\} + [C] \tag{9}$$

$$A_s = [D_s][Na_s]^z \tag{10}$$

Using these equations it is possible to evaluate parameters that have physical meaning in relation to fibre structure. In the first instance a value of 0.45 mL/g was selected for the accessible volume (V) of re-wetted lyocell, based on previous studies using Direct Blue 71 dye [24]. For the purposes of this comparative analysis the accessible volume was assumed to be constant for lyocell. This being the case, the volume could be applied together with carboxyl content for re-wetted lyocell to calculate a value for the free energy of dyeing for each of the five reactive dyes used in the present study. Then, assuming a constant free energy for the cellulose adsorption interaction, an accessible volume (V) could be determined from the model for each dye applied to the five other never-dried and re-wetted fibre samples, again with the necessary corrections for fibre carboxyl contents. The results are shown in Table 3.

The relation between experimental water retention (WR) and model accessible volume (V) is shown for the different dyes in Figs. 5–7. Trend lines from least-squares linear regression have been added for all fibre samples, with correlation coefficient displayed on the graphs, although as will be discussed, the model apparently predicts a higher accessible volume for re-wetted lyocell than expected from the water retention value. This is consistent with the excellent dyeing efficiency of lyocell under commercial conditions. The use of a constant accessible volume for re-wetted lyocell effectively removes the influence of differences in molecular size and shape of the five dyes, which might in reality lead to differing accessibilities. However, this has the useful effect of shifting the data from all dyes to the same reference position, so meaningful averaging of model volumes is possible. A plot of averaged accessible volume (V) against water retention is shown for the different fibre samples in Fig. 7, with re-wetted lyocell excluded from the regression analysis. The trend-line equation is also displayed.

Discussion

The physical adsorption behaviour of all the dyes used in this study is strongly influenced by the total fibre pore volume, as measured either by centrifugation or by solute exclusion. This is expected from the thermodynamic treatment of Peters and Vickerstaff, from Figs. 5–7, which shows that at constant free energy of dyeing there is a

Table 3 Fibre accessible volume and free energy of dyeing calculated from Peters and Vickerstaff model

Dye	Red 120	Red 141	Yellow 84	Orange 84	Navy 171	
Free energy of dyeing (–kJ/mol)	27.3	33.6	27.5	26.0	28.1	
Number of sulphonate groups (z)	6	8	8	8	6	
Purity (wt%)	55	52	46	51	55	
molecular weight	1338	1774	1658	1850	1419	
Fibre type	Modelled accessible volume (V) (mL/g)					Average
Never-dried lyocell	0.59	0.53	0.52	0.58	0.55	0.55
Never-dried viscose	0.62	0.50	0.53	0.56	0.50	0.54
Never-dried modal	0.41	0.32	0.37	0.37	0.33	0.36
Re-wetted lyocell	(0.45)	(0.45)	(0.45)	(0.45)	(0.45)	0.45
Re-wetted viscose	0.50	0.48	0.50	0.50	0.51	0.50
Re-wetted modal	0.33	0.31	0.32	0.37	0.30	0.33

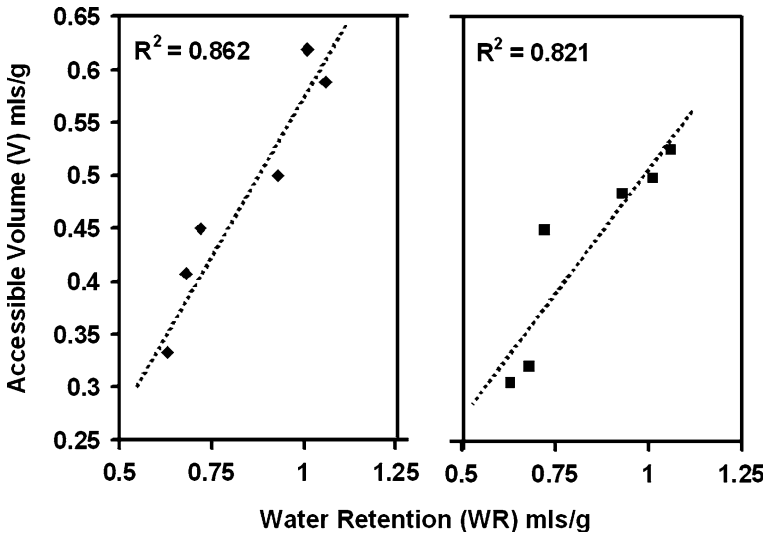

Fig. 5 Relationship between model accessible volume (V) from dye adsorption, and experimental water retention (WR) from centrifugation, for Reactive Red 120 (◆) and Reactive Red 141 (■) dyes

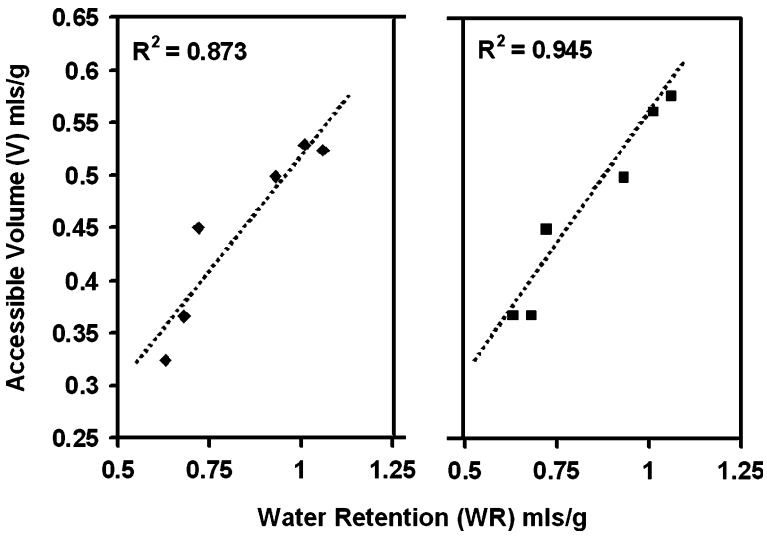

Fig. 6 Relationship between model accessible volume (V) from dye adsorption, and experimental water retention (WR) from centrifugation, for Reactive Yellow 84 (◆) and Reactive Orange 84 (■) dyes

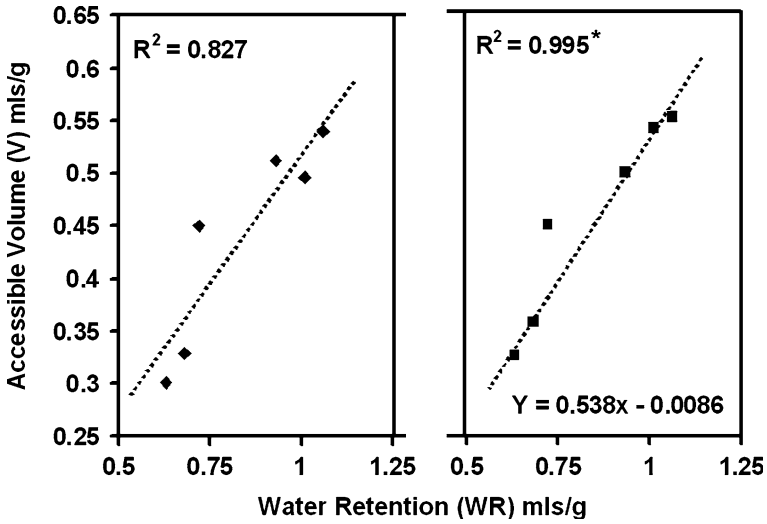

Fig. 7 Relationship between model accessible volume (*V*) from dye adsorption, and experimental water retention (WR) from centrifugation, for Reactive Blue 171 (◆) dye, and the average from all dyes (■). *Re-wetted lyocell excluded from trend

correlation between total pore volume and the modeled accessible volume (*V*). The relationship appears consistent for both never-dried and commercial dried fibre materials, according to Table 3, although re-wetted lyocell is an exception. There are significant differences between the measured fibre carboxyl contents of the three cellulosic variants shown in Table 1, and also reported in the literature [33], which were accommodated in the model predictions. The uptake of anionic dyes is highly sensitive to fibre charge, which in turn influences the thermodynamic equilibration of all ionic species across the fibre/dye-bath boundary [12, 34].

Previous studies have suggested that to a first approximation the nature of the cellulose-dye interaction is universal, regardless of the source of the cellulosic material, so comparisons are valid using a fixed free energy value for each dye [12, 24]. Differences in free energy between dye types are then considered to depend only to depend only on the dye chemical structure. Bae et al. found a value of 26 kJ/mol for Reactive Red 120 applied to cellulose film [11], compared to 27 kJ/mol found in the current study. As discussed, the use of a constant value for accessible volume for re-wetted lyocell has the effect of shifting data for all dyes to the same reference position, allowing sensible averaging. The current dyes and the previously studied dye Direct Blue 71 [24] all have highly planar structures with broadly similar molecular dimensions. This shift is not expected to be of great magnitude and therefore should not have significant impact on the methodology.

Both centrifugation and total solute exclusion techniques reveal that lyocell undergoes a large irreversible reduction in total pore volume between the never-dried and re-wetted condition, a 32% change according to the water retention data in Table 1. This follows the consolidation of the polynosic-type fibrillar structure, where the aligned surfaces of the cellulose domains achieve crystalline register on removal of the intervening water, forming permanent inter-chain hydrogen bonding. The water-promoted coalescence of the fibrillar structure of lyocell has been studied previously using a various physical methods [1, 7, 15, 35–37].

The Peters and Vickerstaff model follows the consolidation of the structure of lyocell, indicating a reduction in accessible volume (*V*) from the never-dried to re-wetted condition for all dyes, shown in Table 3. In contrast, viscose and modal never-dried fibres show a much lower reduction in total pore volume following initial drying, around 7% from the water retention data in Table 1. The corresponding loss of accessible volume predicted by the model is also much lower, according to Table 3. These fibres have a much less organized morphology, with lower orientation and lower crystallinity [38, 39]. The coalescence process may be hindered by the lack of opportunities for alignment of cellulose chains, with no little additional crystallization possible between adjacent cellulose surfaces. The dense nature of the never-dried texture of modal may be at a limit in terms of possible further consolidation [39]. This same dense texture exists around the skin region of viscose and is believed to hinder the uniform collapse of the fibre in the spin-bath [38]. The resulting crenulated appearance of the fibre cross-section is due to the buckling of this layer as it resists the contraction of the less dense internal texture. This same mechanism may contribute to stability of the fibre towards further loss of swelling capacity following initial drying.

A correlation between dye uptake and total pore volume has been verified by a number of previous studies [7, 19], suggesting that this bulk fibre property will give a general prediction of fibre response towards aqueous treatment solutions. This work shows that the re-wetted pore volume of lyocell is below that of viscose, and yet its dye adsorption is greater, most noticeably under low salt dyeing

conditions [4]. The lower anionic charge associated with lyocell will be partly responsible for its enhanced dye uptake, although this is accounted for in the Peters and Vickerstaff model. The model reveals that the underlying accessible volume for re-wetted lyocell is consistently above the trend-line for the other fibres, according to Figs. 5–7.

The solute exclusion experiment can reveal information about the distribution of wet-state pore sizes, and how this may differ between lyocell, viscose and modal type morphologies. The cumulative accessible volume graphs in Figs. 2–4 show that for all fibres there is a conversion from a nascent texture with a spread down to very small pores, to an evolved texture where the pores are apparently of larger size. Whilst at first this seems counter-intuitive, it does follow from the expected process of consolidation following initial drying. If the never-dried phase-separated texture is not at true thermodynamic equilibrium, in a metastable state, then process of drying and rewetting may promote further coarsening, associated with the mechanism of spinodal decomposition [16, 40].

Previous investigations have also shown that the nascent ordered regions of the never-dried structure of lyocell remain hydrated, with water molecules inter-digitated between the $1\bar{1}0$ cellulose planes [1]. These hydrated crystal regions represent a population of very small pores, which may disappear irreversibly on initial drying. This is consistent with the fall in internal surface areas seen for all fibres, according to Table 2. The permanent exudation of crystal water would also contribute to the reduction in swelling capacity of re-wetted lyocell. Viscose and modal may also loose crystal water, although their poorer structural organization may limit this effect. However, water may aid the segmental motion of the disordered polymer regions in these fibres allowing reorganisation of the pore texture. The coarsening mechanism may still be effective, with larger inter-domain pores growing at the expense of smaller intra-crystalline spaces, causing a shift to higher mean size.

The static solute exclusion experiment allows effective equilibrium partitioning of solute probe molecules within the small intra-crystalline spaces of the never-dried fibres, which may be more complete than achieved under dynamic flow conditions. The contribution from these spaces may therefore be underestimated using the high-pressure chromatographic version of the technique [5, 17, 18]. In addition, the presence of a mixed cellulose-water phase may not be accounted for in the two-phase analysis employed in the interpretation of small-angle X-ray scattering data [1, 7].

The accessibility of the solute exclusion probes is to a first approximation governed by the same constraints as the accessibility of the dyes in the adsorption experiment. Both molecule types experience a chemical potential gradient, which encourages diffusion through the channels present in the wet-state fibres. Access to theses internal channels depends on their entrance widths, so molecules with smaller profiles will penetrate into finer spaces than larger molecules. On the basis of PEG/PEO exclusion, the never-dried materials have a lower accessibility in the intermediate to large size range than the re-wetted equivalents, for all fibre variants. On the other hand, the dye adsorption of the never-dried fibres is typically greater than the re-wetted fibres. This contradicts the assumption that it is the availability of larger size channels which is important for dye molecule accessibility and which dictates dyeing efficiency. On the same basis the dye adsorption of re-wetted lyocell should be lower than that of viscose.

Several explanations for these anomalies may exist. First, it is evident that typical reactive and direct dyes do not have the globular shapes that are adopted by PEG/PEO in solution. Planar aromatic dyes have a narrow dimension across the ring plane, which may increase their freedom for diffusion through the asymmetric internal channels of the fibres. This may especially be the case for re-wetted lyocell, where the inter-fibrillar pore channels are themselves assumed to have a planar (lamellar) geometry. Also, dye molecules are strongly adsorbed and may diffuse by a series of exchanges between the internal solution and the internal channel surfaces. The need for full three-dimensional tumbling may not exist, the dye motion being quite different to that of non-adsorbed flexible molecule such as PEG/PEO. The possibility of surface-translation type diffusion may also assist the access of dyes molecular into the small asymmetric spaces within the fibre structure. The strong adsorption forces may even encourage planar dyes to develop cooperative interactions within very small spaces at both dye faces. Such complexes have been described where planar dyes been found to inter-digitate between the $1\bar{1}0$ crystalline planes of a growing bacterial cellulose culture [41].

The good correlation between the model accessible volume and total fibre porosity may also be a result of the influence of the other mobile ions within the cellulosic structure. The ionic product in Eq. 8 depends on the z-power of the sodium concentration in the fibre, which must be converted to a molar basis by division using a volume term also raised to the z-power. This volume relates to the space available to the sodium rather than the large dye ions. Allowing for charge separation, the sodium ions may actually be able to explore a greater proportion of the total pore volume than the dye anions. The volume calculated from the model would be weighted towards the sodium ion accessibility, which would include the contribution from of the smallest pores identified in the solute exclusion experiment. A revised Eq. 11 may be more appropriate for future studies, where V_D is the dye accessibility and V_{Na} is

the sodium accessibility. A revision to Eq. 9 may also be considered, although both these modifications will lead to greater difficulties in model fitting.

$$A_f = \frac{[D_f][Na_f]^z}{V_D.V_{Na}^z} \quad (11)$$

From the dye adsorption study, the re-wetted lyocell sample displays a higher accessible volume than predicted from its total pore volume. As discussed, this may relate to its more ordered fibrillar texture, characteristic of the air-gap draw employed in the manufacture of the fibre [42–44]. In the never-dried state the surfaces of the fibrillar domains are exposed, comprised of layers of hydroxyl groups projecting into the internal solution. These surfaces will interact efficiently with incoming planar dye molecules, regardless of consideration of the specific mechanisms for adsorption. The consolidation of the structure on initial drying may improve the uniformity of these fibrillar surfaces, which will be exposed again on re-wetting. This may lead to an increase in the number of effective surface-dye interactions, whilst the intrinsic free energy of dyeing may still be considered constant [12, 24]. A separate consideration of the internal surface area available for interactions may be necessary for a fully robust prediction of dye uptake, although this may not be derived concurrently with the accessible volume [13, 45]. The fibre internal surface area is not accounted for by the Peters and Vickerstaff model, which includes all accessibility effects within the single volume parameter. Related dye isotherm studies have shown that the free energy of dyeing is reduced when the cellulose internal surfaces are disrupted by fixation of resin chemicals [46]. Ultimately, the magnitude of the dye-cellulose interaction may depend on the stereo-chemistry of the internal cellulose surfaces as well as that of the dye [24, 47].

Conclusions

The experimental wet-state pore volumes of a series of cellulosic fibres have been shown to correlate with the accessible volume described in the thermodynamic model of Peters and Vickerstaff, adding physical significance to the concept of an internal fibre solution. The model has been applied to interpret the adsorption behaviour of typical reactive dyes and has been successful in accounting for differences in fibre anionic charge and the presence of electrolyte ions in the dye solution.

Solute exclusion data suggests the presence of a population of very small spaces in viscose, modal and lyocell never-dried fibres, which may be associated with water disrupting the cellulose $1\bar{1}0$ crystal planes. Such intra-crystalline spaces may allow access to highly planar substantive dyes. In addition these spaces may also be accessible to sodium ions, which may lower the chemical potential of the dye and counterions in the internal solution and so enhance dye adsorption.

Lyocell shows a large reduction in total wet capacity following initial drying, which is presumed to be due to both exudation of crystal water and to inter-fibrillar crystallisation. The mechanism of inter-domain crystallisation may not be so effective for viscose and modal, which have poorer structural organization. Re-wetted lyocell shows unusually high dye adsorption, as the uniformity of the inter-fibrillar pore surfaces of this fibre may permit greater numbers of effective interactions with incoming planar dyes.

Acknowledgements The authors would like to thank The Christian Doppler Society for financial support, and also Lenzing AG, for financial support and for supply of fibre samples. Thanks also to Dr Christian Schuster for helpful discussions.

References

1. Weigel P, Fink H-P, Walenta E, Ganster J, Remde H (1997) Cell Chem Technol 31:321
2. Kaenthong S, Phillips SAD, Renfrew AHM, Wilding AM (2005) Colouration Technol 120(6):316
3. Bredereck K, Stefani H-P, Beringer J, Schulz F, Commarmot A (2003) Melliand Textilberichte 84(1–2):58
4. Kaenthong S, Phillips SAD, Renfrew AHM, Wilding AM (2005) Colouration Technol 121(1):45
5. Bredereck K, Gruber M, Utterbach A, Schulz F (1996) Textilveredlung 31:1
6. Vickerstaff T (1954) The physical chemistry of dyeing, Chap VII. Oliver and Boyd, London
7. Vickers ME, Briggs PN, Ibbett RN, Payne J, Smith SB (2000) Polymer 42:241
8. Abbott LC, Batchelor NS, Jansen L, Oakes J, Lindsay-Smith RJ, Moore NJ (2004) New J Chem 28(7):815
9. Sivaraja SR, Srinivasan G, Baddi TN (1968) Textile Res J (July):693
10. Sasaki H, Donkai N, Takagishi T (2004) Textile Res J 74(6):509
11. Bae S-H, Motomura H, Morita Z (1997) Dyes Pigments 34(1):37
12. Marshall WJ, Peters HR (1947) J Soc Dyers Colourists 63:446
13. Daruwalla HE, D'Silva AP (1963) Textile Res J 59:40
14. Sivarajalyer SR, Raghunath R (1989) Proc Natl Acad Sci India Sec A Phys Sci 59(1):37
15. Crawshaw J, Cameron ER (2000) Polymer 41(12):4691
16. Moss CE, Butler EC, Muller M, Cameron RE (2002) J Appl Polym Sci 83:2799
17. Bredereck K, Gruber M (1995) Melliand Textilberichte 76:684
18. Bredereck K, Schulz F, Otterbach A (1997) Mellian Textilberichte 78(10):103
19. Bredereck K, Saafan A (1981) Die Angewandte Makromolekulare Chemie 95:13 (Nr. 1482)
20. Stone EJ, Scallan MA (1968) Cellulose Chem Technol 2:343
21. Stone EJ, Scallan MA, Abrahamson B (1968) Svensk Papperstidning 71(19):187
22. Peters RH, Vickerstaff T (1948) Proc Roy Soc (Lond) A192:292
23. Carillo F, Lis JM (2002) Dyes Pigments 53:129
24. Ibbett RN, Phillips AD, Kaenthong S (2006) Dyes Pigments 71:168

25. Murtagh V, Taylor AJ (2004) Dyes Pigments 63:17
26. Morton WE, Hearle SWJ (1993) Physical properties of textile fibres, 3rd edn, Chap 10. William Heinemann Ltd, in association with The Textile Institute
27. Davidson GF (1948) J Textile Inst 39:T65
28. Kaewprasit C, Hequet C, Abidi N, Gourlot J-P (1998) J Cotton Sci 2:164
29. Lin KJ, Ladisch HM, Patterson AJ, Noller HC (1987) Biotechnol Bioeng 29:976
30. Gamma MF, Teixeira AJ, Mota M (1994) Biotechnol Bioeng 43:381
31. Squire PG (1981) Chromatogr J 210:433
32. Dork L, Sahagian D, Proussevitch A (1998) J Volcanol Geoth Res 84:173
33. Fras L, Laine J, Stenius P, Stana K-Kleinschek, Ribitsch V, Dolece V (2004) J Appl Polym Sci 92:3186
34. McGregor R (1972) Textile Res J 68:536
35. Fink H-P, Weigel P, Purs JH, Ganster J (2001) Prog Polym Sci 26:1473
36. Dube M, Blackwell HR (1983) TAPPI Proceedings of the international conference on dissolving and speciality pulps, Jan 1983
37. Bredereck K (2005) Rev Prog Colouration 35:39
38. Peter H, Priest MH (1968) In: Mark HF, Atlas SM, Cernia E (eds) Man-made fibers: science and technology, Vol II, Chap 2. Interscience Publishers, New York
39. Moncrief WR (1970) Man-made fibres, 5th edn, Chap 13. Haywood Books, London
40. Fujita H (1990) Polymer solutions: studies in polymer science, Vol 9, Chap 10.2. Elisvier BV
41. Ibrahim MD, Mondal H, Akira K (2001) . J Appl Polym Sci 79:1726
42. Franks EN, Varga JK (1980) US Patent No. 4,196, April 1980, 282
43. Lenz J, Schurz J, Eichinger D (1994) Lenziner Berichte 9:19
44. Lenz J, Schurz J, Wrentschur E (1992) Acta Polym 43:12
45. Porter JJ (1993) Textile Chemist Colourist 25:4
46. Yang Y, Lan T, Li S (1995) Textile Chemist Colourist 27(2):29
47. Ibbett RN, Phillips AD, Kaenthong S (available online 28th Sept 2006) Dyes Pigments